

# Dissolution kinetics and behavior of $\delta$ phase in Inconel 718<sup>①</sup>

CAI Dayong(蔡大勇), ZHANG Weihong(张伟红), NIE Purin(聂璞林),  
LIU Wenchang(刘文昌), YAO Mei(姚 枚)

(Key Laboratory of Metastable Materials Science and Technology,  
Yanshan University, Qinhuangdao 066004, China)

**Abstract:** Dissolution kinetics of  $\delta$  phase in Inconel 718 at 980, 1 000 and 1 020 °C respectively was established using the quantitative X-ray diffraction(XRD) method. Microstructure evolution during dissolution process was analyzed with scanning electron microscopy(SEM). Dissolution rate of  $\delta$  phase during high temperature heating keeps at a high level at the beginning stage, and then decreases gradually with the increase of heating time. A dynamic equilibrium state approaches after being heated at 980 °C for more than 30 min and at 1 000 °C for more than 2 h, and the equilibrium mass fraction are 3% and 0.6% respectively.  $\delta$  phase fully dissolves into the austenitic matrix after being heated at 1 020 °C for more than 2 h. The dissolution and fracture effects cause the morphology evolution of  $\delta$  phase from long needle shape to short bars or particles at high temperature.

**Key words:** Inconel 718;  $\delta$  phase; dissolution kinetics; diffusion

**CLC number:** TC 113.12

**Document code:** A

## 1 INTRODUCTION

Ni-Fe base superalloy Inconel 718, which is age-hardened by combined precipitation of fine  $\gamma'$  and  $\gamma''$  phases in austenitic matrix, has been widely used for high temperature services such as gas turbine disks. The amounts of precipitation phases together with their shape and distribution have determinant influence on the mechanical properties of Inconel 718. The precipitation of intermetallic phases in Inconel 718 has been intensively studied<sup>[1, 2]</sup>. It has been found that the major hardening phase is  $\gamma''$ , and  $\delta$  is the equilibrium phase. All these three phases are of the A<sub>3</sub>B type: the  $\gamma''$  and  $\delta$  phases are based on the composition of Ni<sub>3</sub>Nb and the  $\gamma'$  phase on the Ni<sub>3</sub>(AlTi). The precipitation of  $\delta$  phase is always preceded by  $\gamma'$  and  $\gamma''$  precipitation in the low temperature range (below 900 °C), and always occurs in the approximate temperature range of 750 - 1 050 °C. The  $\delta$  phase can precipitate directly from the supersaturated  $\gamma$  matrix if the treatment is carried out at 900 - 1 000 °C<sup>[3-5]</sup>. Contrary to the behaviors of  $\gamma'$  and  $\gamma''$ , the  $\delta$  phase seems to have a beneficial effect on stress rupture ductility. Controlled precipitation of the  $\delta$  phase at grain boundary is believed to have beneficial effect on the stress rupture ductility, and can also inhibit the growth tendency of austenitic grain during forging process<sup>[6-9]</sup>. During hot working such as forging, the  $\delta$  phase may partially dissolve in

to the austenitic matrix. So controlling the precipitation and dissolution of  $\delta$  phase is the most important aspect. But little work has been performed in the latter aspect.

The aims of this work are to analyze the dissolution kinetics and behavior of  $\delta$  phase at evaluated temperatures.

## 2 EXPERIMENTAL

### 2.1 Materials and heat treatment

Hot rolled bars of Inconel 718 were selected for the dissolution behavior analysis and the average grain size was about 20  $\mu$ m. The chemical composition is listed in Table 1. Solid solution treatment was performed at 980 °C for 3 h and then followed by air cooling. The  $\delta$  phase ageing treatment (heating at 890 °C for 20 h) was carried out to insure adequate amount of  $\delta$  phase in the austenitic matrix for dissolution analysis. Dissolution treatment was performed at 980, 1 000 and 1 020 °C, respectively.

**Table 1** Chemical compositions of Inconel 718 alloy (mass fraction, %)

C	Cr	Ti	Ni	Mo	Nb+ Ta	
0.032	18.8	1.05	53.28	2.97	5.12	
Al	B	Fe	Mn	Si	S	P
0.58	0.002	Bal.	0.13	0.09	0.002	0.005

① **Foundation item:** Project(59971039) supported by the National Natural Science Foundation of China

**Received date:** 2002 - 10 - 22; **Accepted date:** 2003 - 02 - 20

**Correspondence:** CAI Dayong; Tel: + 86-335-8074729; Fax: + 86-335-8051148; E-mail: dayongcai@sina.com.cn

## 2.2 X-ray diffraction quantitative phase analysis and microstructure observation

According to the phase transformation specialties of Inconel 718,  $\gamma$  phase,  $\delta$  phase and NbC are the main three phases after dissolution treatment. The amount of  $\delta$  phase can be directly determined using X-ray diffraction (XRD) technique from comparison of the integrated intensity of the diffraction peaks<sup>[10]</sup>.

Microstructure evolution during dissolution process was observed by KYKY 2800 SEM.

## 3 RESULTS AND DISCUSSION

### 3.1 Dissolution kinetics of $\delta$ phase in Inconel 718

To establish the dissolution kinetics of  $\delta$  phase in Inconel 718, the amounts of  $\delta$  phase during dissolution process are defined. Fig. 1 shows the calculated  $w_t/w_0-t$  profiles for different dissolution temperatures, where  $w_0$  is the initial mass fraction;  $w_t$  is mass fraction at any instant during dissolution process. Three different dissolution stages can be found during heating at 980 and 1 000 °C, and two stages at 1 020 °C. The first stage occurs at the beginning of dissolution process, during which the dissolved amount of  $\delta$  phase is linear with the heating time. Dissolution rate keeps nearly constant and at a high level in this stage. The second one is characterized as a parabolic type between dissolved amount and time. In this stage, dissolution rate decreases gradually with the proceeding of dissolution process, and high dissolution rate accompanies with high heating temperature at the same instant. The dissolution process finishes at the end of the second stage at 1 020 °C, and  $\delta$  phase fully dissolves into the matrix. By contrast, another linear stage appears at 980 and 1 000 °C, and dissolution rate keeps at a nearly constant value 0. In other words, the dissolution process ends with the coming of a dynamic equilibrium state and the corresponding equilibrium mass fraction of  $\delta$  phase are 3% and 0.6% respectively.

The above results are input into Origin 6.0 for further processing. An empirical relation between  $w_t/w_0$  and heating time  $t$  is obtained as Eqn. (1). Values of the corresponding parameters are listed in Table 2.

$$w_t/w_0 = B + \frac{A}{\pi} \cdot \frac{m}{4(t-t_0)^2 + m^2} \quad (1)$$

**Table 2** Parameters in Eqn. (1)

Dissolution temperature/ °C	B	A	m	$t_0$
980	35.3	14.2	0.13	- 0.02
1 000	12.3	152	0.08	- 0.14
1 020	4.23	157	0.07	- 0.13

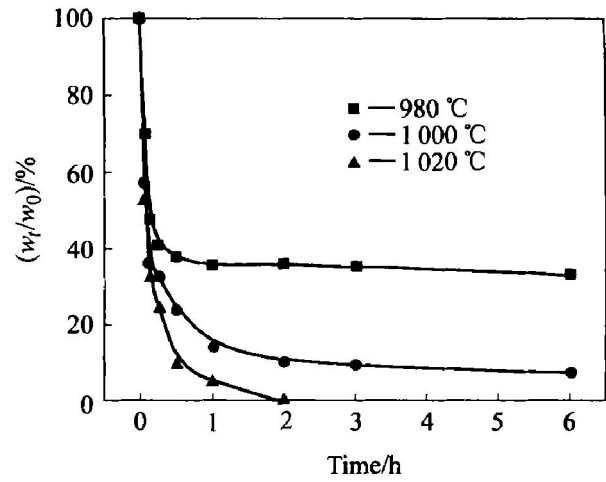


**Fig. 1** Dissolution kinetics of  $\delta$  phase in Inconel 718

where  $A$ ,  $B$ ,  $m$  and  $t_0$  are constants,  $t$  is holding time at a certain temperature.

The dissolution process of  $\delta$  phase in Inconel 718 is controlled by the diffusion of Nb atoms in the austenitic matrix. The diffusion process proceeds in two sequence steps. One is a short distance migration of atoms from one side of phase boundary adjacent to  $\delta$  phase to the other side adjacent to austenitic matrix<sup>[11]</sup>. The flux  $J_B$  of atoms across the phase boundary is determined by the boundary migration rate  $M$  and migration driving force  $\Delta\mu_B$ , which can be described by Eqn. (2)

$$J_B \propto M \cdot \Delta\mu_B \quad (2)$$

The other step is a long distance diffusion process of atoms from the phase boundary adjacent to matrix to the austenitic matrix, and the flux  $J'_B$  of atoms is controlled by the coefficient of cubic diffusion and concentration gradient between phase boundary and matrix. This process can be expressed by Eqns. (3) and (4)

$$J'_B = D \left( \frac{\partial c_B}{\partial x} \right) \quad (3)$$

$$D = D_0 \exp\left(-\frac{Q}{RT}\right) \quad (4)$$

where  $D_0$  and  $Q$  are frequency factor and activation energy respectively.

Between the two diffusion steps, the slow one is the controlling step. The boundary migration rate  $M$  in Eqn. (2) is dependent upon the accommodation probability when atoms migrate from one side of phase boundary adjacent to  $\delta$  phase to the other side adjacent to matrix. The accommodation probability, also defined as carrying factor, is mainly determined by the structure of phase boundary. The interface between  $\delta$  phase and matrix in Inconel 718 is incoherent, where atoms are in disarrangement. So the accommodation position has little influence on migration process of atoms from one side of the phase boundary to the other, and the carrying factor is close to 1. Ac-

According to the adequate migration rate of phase boundary, the whole dissolution process is determined by the long distance diffusion process of atoms from the phase boundary to the matrix.

As described in Eqns. (3) and (4), the main factors affecting the diffusion process are concentration gradient and temperature. Due to the high concentration gradient, the dissolution process of  $\delta$  phase proceeds with high and nearly constant rate at the beginning stage. The concentration gradient decreases gradually with the proceeding of dissolution process; meanwhile, dissolution rate decreases. An equilibrium diffusion state will reach with a certain amount of  $\delta$  phase in the matrix at 980 and 1 000 °C, so the dissolution rate is equal to 0. Also temperature has decisive effects on the diffusion process. That the dissolution rate increases with the increase of temperature can be interpreted by the high diffusion coefficient at high temperature. Also it should be noted that high temperature should be accompanied with high solid solubility of Nb atoms in matrix, so the  $\delta$  phase can fully dissolve at 1 020 °C.

### 3.2 Morphology evolution of $\delta$ phase during dissolution process

Fig. 2 shows the morphology evolution of  $\delta$  phase during high temperature heating process. Large amount of long needle-like  $\delta$  phase exist in the austenitic matrix at ageing state before dissolution process (Fig. 2(a)), and then it gradually dissolves into the matrix (Fig. 2(b)). Meanwhile, the long needle-like  $\delta$  phase breaks into pieces and transforms into short bars or particles (Figs. 2(c) and (d)). Microstructure evolution indicates the

same characteristics during heating at different temperatures. Large amount of  $\delta$  phase, existing as short bars or particles, still distribute in the austenitic grains and along grain boundaries when being heated at 980 °C for 6 h, and the grain size changes little. On the contrary, the amount of  $\delta$  phase decreases obviously after being heated at 1 000 and 1 020 °C, and the austenitic grain size increases (Figs. 2(e) and (f)).

Relationship between the solubility of secondary phase and its curvature was proposed by the colloidal state equilibrium law<sup>[12]</sup>. Generally, the particles with high curvature have high solubility. Regarding the long needle-like  $\delta$  phase in Inconel 718, the solubility at the point end is higher than that at the face. So the concentration of Nb atoms in the matrix adjacent to the point end is higher than that in the matrix adjacent to the face. Thus, the concentration difference caused by diffusion in the matrix destroys the concentration equilibrium state of Nb atoms among the phase interfaces. In order to reach a new equilibrium state, further dissolution of  $\delta$  phase continues. The above process proceeds repeatedly until a dynamic equilibrium state comes. Moreover, subgrain boundary or high density dislocation zone might exist in the  $\delta$  phase, where dissolution occurs preferentially. As a result, channels will appear at the defect locations accompanying with the dissolution process. Because of the difference of curvature between the channel and other faces, dissolution rate difference increases between the channel zone and plane position. As a result, the  $\delta$  phase will dissolve gradually and fracture from the defect zone. The dissolution and fracture schematics of  $\delta$  phase is shown in Fig. 3. The above dissolution and fracture effect

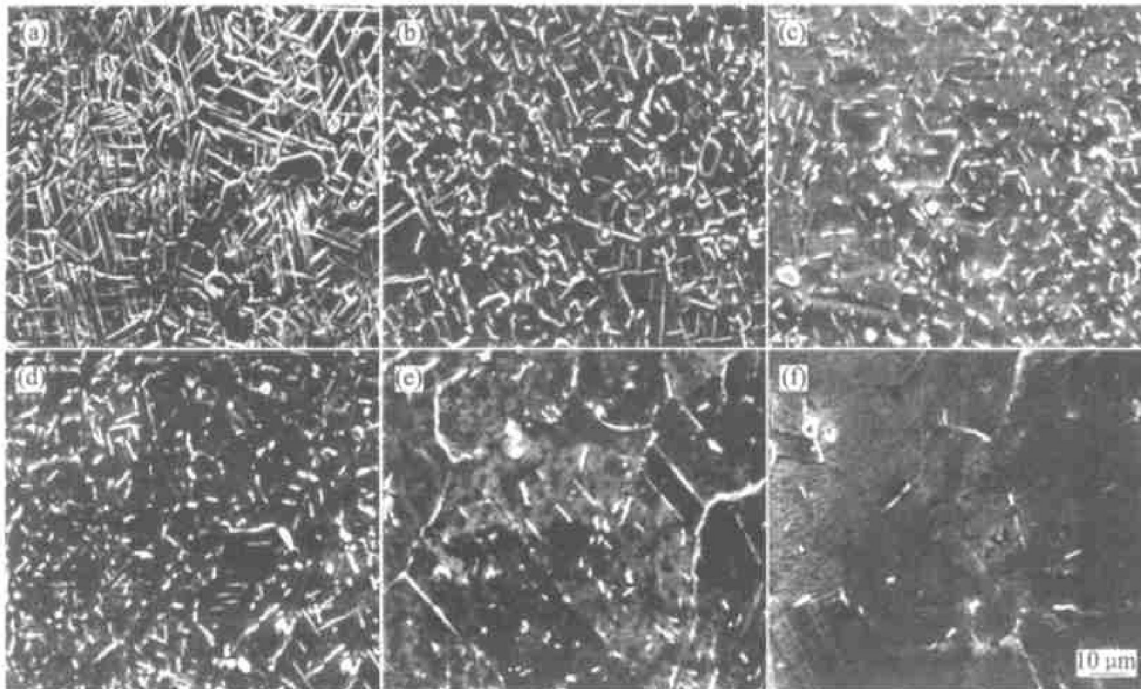


**Fig. 2** Morphology evolution of  $\delta$  phase in Inconel 718 during dissolution process

(a) —Ageing state; (b) —980 °C, 1 h; (c) —980 °C, 2 h; (d) —980 °C, 6 h; (e) —1 000 °C, 2 h; (f) —1 020 °C, 1 h

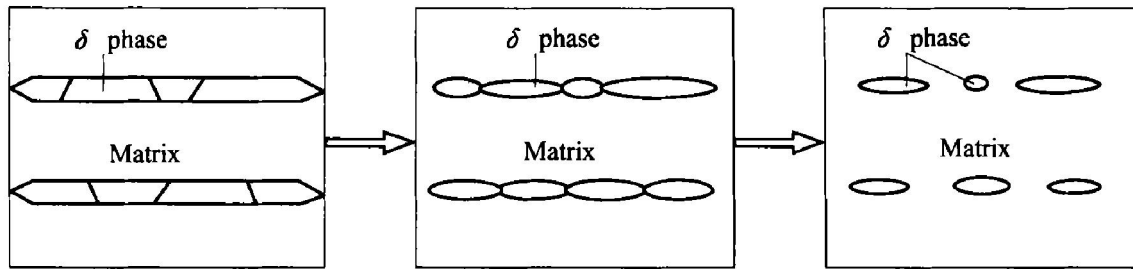


**Fig. 3** Schematics of dissolution and fracture process of  $\delta$  phase in Inconel 718

will cause the morphology evolution of  $\delta$  phase from long needle shape to short bars or particles.

#### 4 CONCLUSIONS

1)  $\delta$  phase can fully dissolve into the austenitic matrix after being heated at 1 020 °C for more than 2 h. A certain amount of  $\delta$  phase still exist after being heated at 980 and 1 000 °C for more than 6 h respectively.

2) Dissolution rate keeps at a high level at the beginning stage, and then decreases gradually with the increase of heating time. A dynamic equilibrium state approaches after being heated at 980 °C for more than 30 min and at 1 000 °C for more than 2 h respectively.

3) The dissolution and fracture effects cause the morphology evolution of  $\delta$  phase from long needle-like shape to short bars or particles.

#### REFERENCES

- [ 1 ] Sundararaman M, Mukhopadhyay P, Banerjee S. Some aspects of the precipitation of metastable intermetallic phases in Inconel 718[J]. Metall Mater Trans A, 1992, 23A: 2015 - 2028.
- [ 2 ] Dedvallees Y, Bouzidi M, Bois F, et al. Delta phase in Inconel 718: mechanical properties and forging process requirements[A]. Loria E A. Superalloys 718, 706 and Various Derivatives[C]. TMS, 1994. 281 - 291.
- [ 3 ] Krueger D D. The development of direct age 718 for gas turbine aging disk applications[A]. Loria E A . Superalloy 718-Metallurgy and Application[C]. TMS, 1989. 279 - 296.
- [ 4 ] Han Y F, Deb P, Chaturvedi M C. Coarsening behavior of  $\gamma''$  and  $\gamma'$  particles in Inconel 718[J]. Metal Sci, 1982, 16: 555 - 561.
- [ 5 ] Lim A W, Zhuang J Y, Yang J Y, et al. The effect of phase on crack propagation under creep and fatigue conditions in alloy 718[A]. Loria J Y. Superalloys 718, 625, 706 and Various Derivatives[C]. TMS, 1994. 545 - 549.
- [ 6 ] Dix A W, Hyzak A W, Singh A W. Application of ultra fine grain alloy 718 forging billet[A]. Antolovich A W. Superalloys 1992 [C]. TMS, 1992. 23 - 32.
- [ 7 ] Sundararaman M, Kishore R, Mukhopadhyay P. Strain hardening in underaged Inconel 718 [J]. Metall Mater Trans A, 1994, 25A: 653 - 656.
- [ 8 ] GENG Lin, ZHENG Zhe-zhu, NA Yong-song, et al. Effect of thermal exposure on precipitation behavior and hardness of alloy 718[J]. Trans Nonferrous Met Soc China, 2000, 10(3): 340 - 344.
- [ 9 ] LIU Weir-chang, YAO Mei, CHEN Zhong-lin. Niobium segregation in Inconel 718[J]. J Mater Sci, 1997, 10: 213 - 216.
- [ 10 ] LIU W C, XIAO F R, YAO M, et al. Relationship between the lattice constant of  $\gamma$  phase and the amount of  $\delta$  phase,  $\gamma''$ , and  $\gamma'$  phase in Inconel 718[J]. Scripta Materialia, 1997, 37: 59 - 64.
- [ 11 ] Ahn S, Kang S. Effect of various carbides on the dissolution behavior of Ti( $C_{0.7}N_{0.3}$ ) in a Ti( $C_{0.7}N_{0.3}$ )-30Ni system [J]. International Journal of Refractory & Hard Materials, 2001, 19: 539 - 545.
- [ 12 ] Björneklett B I, Grong  $\delta$ , Myhr O R. Additivity and isokinetic behavior in relation to particle dissolution [J]. Acta Mater, 1998, 46(17): 6257 - 6266.

( Edited by YANG Bing)